

## CHAPTER 66

### Quasi-Three-Dimensional Model for Storm Surges and Its Verification

Takao Yamashita<sup>1</sup>, Yoshito Tsuchiya, M.ASCE<sup>2</sup> and Hiroshi Yoshioka<sup>1</sup>

#### Abstract

Three-dimensional model for storm surges was developed, in which momentum equations first were solved in the vertical direction together with mass conservation and turbulence model, then mass conservation in the horizontally two-dimensional coordinates was solved by the finite difference method. Several fundamental tests concerning swing and wind-induced current, were performed to examine the model properties. Finally the hindcasting of the current profile in the Tanabe bay was conducted to test model applicability.

#### Introduction

Storm surge models have been developed as a two-dimensional model, which is called a vertical integrated model or one(single) level model. Because of Japan's recent need for waterfront development, significant environmental problems and coastal disasters will persist during accelerated future developments in the coastal ocean. It is desired to develop a more sophisticated numerical model for storm surges which predicts the profile of current, turbulence, and surge heights. A three dimensional model for tide and storm surges combined with a turbulence and wind-wave prediction model may become popular in coastal ocean assessment in the near future.

Heaps (1973) studied dynamic response of the Irish Sea to a stationary wind stress field by a finite difference model which solves the homogeneous hydrodynamic equations taken in linearized form by transforming them to eliminate the vertical coordinate  $z$ . The system including the coordinates  $x, y, t$ , and  $z$  was solved by an explicit finite difference scheme. This model only considers homogeneous systems, and neglects the convection terms. A series of numerical experiments was also performed with the model to determine the steady state circulation of the Irish Sea system. Sundermann (1974) and Laevastu (1975) extended the method for three dimensional, multi-level, and multi-layer flow systems. Simons (1974 & 1975) studied the circulation in Lake Ontario under strong stresses by

---

<sup>1</sup>Instructor, Disaster Prevention Research Institute, Kyoto University, Uji, Kyoto, 611 Japan

<sup>2</sup>Professor Emeritus of Kyoto University & Professor, Meijyo University, Tenpaku-ku, Nagoya, 467 Japan

using a four layer model. Sundermann (1974) extended Hansen's (1962) basic two dimensional scheme to study three dimensional tidal circulation of the North Sea. This extension involves an assumption of homogeneous density distributions. The basic two-dimensional explicit scheme of Hansen (1962) also has been extended by Laevastu (1975) by using multi-layer modeling.

Another three-dimensional model which is the simple version of  $\sigma$ -coordinates was developed by Koutitas and O'Connor (1980), in which momentum equations together with mass conservation equation and turbulence model first are solved in the vertical direction. Then mass conservation in the horizontally two-dimensional coordinates is solved. This model elaborates on the vertical motion of fluid and reducing the matrix of difference equations.

Numerical prediction in shallow bays or estuaries must be focused to develop an effective three-dimensional model for environment assessment in the coastal ocean, since this is our most probable development space in the coming century. In this paper, a quasi-three-dimensional (Q3-D) model is developed based on Koutitas and O'Connor's (1980) modeling.

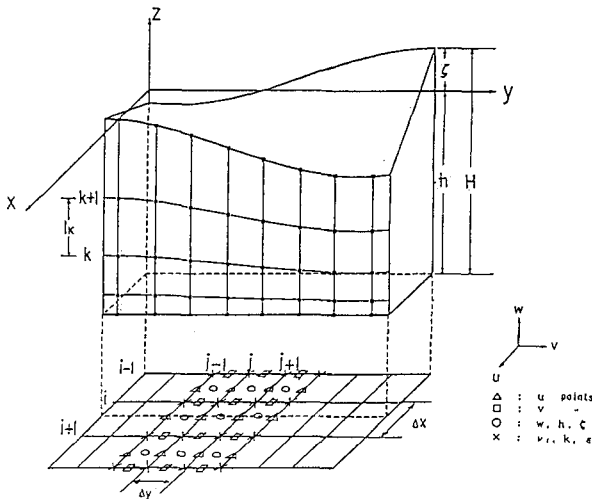


Figure 1 Coordinate system and definition of variables.

### Basic Equations and Solution Method

The basic equations for the Q3-D model consist of the momentum equations of mean flow, the equation of continuity and the equations of turbulence model. The following additional relations for the vertical velocity  $w$  and the surface elevation  $\zeta$  are used.

$$w(x, y, z) = -\frac{\partial}{\partial x} \int_{-h}^z u dz - \frac{\partial}{\partial y} \int_{-h}^z v dz \tag{1}$$

$$\frac{\partial \zeta}{\partial t} + \frac{\partial(HU)}{\partial x} + \frac{\partial(HV)}{\partial y} = 0 \tag{2}$$

which is derived from the mass continuity equation by integrating in the vertical direction. This equation satisfies total mass conservation in the horizontally two-dimensional system.

Vertical distribution of turbulence has to be specified to simulate the velocity distribution of wind-induced mean currents. Several turbulence models are now available for the Q3-D modeling: (1) The so-called zero equation model in which the vertical eddy viscosity  $\nu_t$  is assumed. (2) Multi-equation models in which turbulence kinetic energy budget is described by the standard  $k-\epsilon$  model. In order to get an efficient numerical solution to the three-dimensional system of equations, Koutitas and O'Connor (1980) employed a time fractional finite difference method in which advection and propagation are split. The computational domain is covered by a rectangular-grid system in the  $x-y$  plane, and the water depth is divided into a several layer-elements as shown in Figure 1. The finite element Galerkin method is applied to the momentum equations to obtain nodal velocities over the depth. For the depth-averaged continuity equation (2), the finite difference method is applied.

Applying an explicit scheme, the difference equation of the momentum equation in the  $x$ -direction is written as:

$$\begin{aligned} \frac{u^{n+1} - u^n}{\Delta t} &= -u^n \frac{\partial u^n}{\partial x} - v^n \frac{\partial u^n}{\partial y} - w^n \frac{\partial u^n}{\partial z} - g \frac{\partial \zeta^{n+1/2}}{\partial x} \\ &+ \frac{\partial}{\partial x} \left( \nu_T \frac{\partial u^n}{\partial x} \right) + \frac{\partial}{\partial y} \left( \nu_T \frac{\partial u^n}{\partial y} \right) + \frac{\partial}{\partial z} \left( \nu_T \frac{\partial u^{n+1}}{\partial z} \right) + f v^n \end{aligned} \quad (3)$$

The  $y$ -momentum equation can be shown by the same manner.

Assuming fractional time step  $t^*$ , the momentum equations can be split up as; for the  $x$ -momentum equation,

$$\frac{u^*}{\Delta t} = \frac{u^n}{\Delta t} - u^n \frac{\partial u^n}{\partial x} - v^n \frac{\partial u^n}{\partial y} - w^n \frac{\partial u^n}{\partial z} - g \frac{\partial \zeta^{n+1/2}}{\partial x} \quad (4)$$

$$\frac{u^{n+1}}{\Delta t} - \frac{\partial}{\partial z} \left( \nu_T \frac{\partial u^{n+1}}{\partial z} \right) = \frac{u^*}{\Delta t} + \frac{\partial}{\partial x} \left( \nu_T \frac{\partial u^n}{\partial x} \right) + \frac{\partial}{\partial y} \left( \nu_T \frac{\partial u^n}{\partial y} \right) + f v^n \quad (5)$$

for the  $y$ -momentum equation,

$$\frac{v^*}{\Delta t} = \frac{v^n}{\Delta t} - u^n \frac{\partial v^n}{\partial x} - v^n \frac{\partial v^n}{\partial y} - w^n \frac{\partial v^n}{\partial z} - g \frac{\partial \zeta^{n+1/2}}{\partial y} \quad (6)$$

$$\frac{v^{n+1}}{\Delta t} - \frac{\partial}{\partial z} \left( \nu_T \frac{\partial v^{n+1}}{\partial z} \right) = \frac{v^*}{\Delta t} + \frac{\partial}{\partial x} \left( \nu_T \frac{\partial v^n}{\partial x} \right) + \frac{\partial}{\partial y} \left( \nu_T \frac{\partial v^n}{\partial y} \right) - f u^n \quad (7)$$

and the vertical velocity  $w$  is calculated by

$$w(x, y, z) = -\frac{\partial}{\partial x} \int_{l_k} u(x, y, z) dz - \frac{\partial}{\partial y} \int_{l_k} v(x, y, z) dz \quad (8)$$

The finite element Galerkin method is applied to Eqs. (4) to (7) to solve the nodal velocities over the depth. Substituting the approximated velocity  $\tilde{u}$  into

the original momentum equation and integrating it between nodal points over a whole area, we get the following residual equation in the  $x$ -direction.

$$\int \tilde{u} \frac{u^*}{\Delta t} dz = \int \tilde{u} \frac{u^n}{\Delta t} dz - \int \tilde{u} u^n \frac{\partial u^n}{\partial x} dz - \int \tilde{v} v^n \frac{\partial u^n}{\partial y} dz - \int \tilde{w} w^n \frac{\partial u^n}{\partial z} dz - \int \tilde{u} \frac{\partial \zeta^{n+1/2}}{\partial x} dz \quad (9)$$

Applying this relation to Eqs. (4) to (7), a set of linear equations can be reduced to

$$\left. \begin{aligned} \mathbf{A} \mathbf{u}^* &= \mathbf{a}^n, & \mathbf{B} \mathbf{u}^{n+1} &= \mathbf{b}^* \\ \mathbf{C} \mathbf{v}^* &= \mathbf{c}^n, & \mathbf{D} \mathbf{v}^{n+1} &= \mathbf{d}^* \end{aligned} \right\} \quad (10)$$

where  $\mathbf{A}$  is the  $2 \times 2$  matrix,  $\mathbf{B}$  the  $2 \times 4$  matrix,  $\mathbf{a}$  and  $\mathbf{c}$  are two component vectors, and  $\mathbf{b}$  and  $\mathbf{d}$  are four component vectors.

The linear interpolation function is used as

$$u = N_k u_k + N_{k+1} u_{k+1} \quad (11)$$

where

$$N_k = \frac{1}{l_k} (z_{k+1} - z), \quad N_{k+1} = \frac{1}{l_k} (z - z_k) \quad (12)$$

where  $l_k$  is the element length defined by  $l_k = z_{k+1} - z_k$ .

The three-dimensional current field is obtained by computing these equations which can be solved by the Gaussian elimination method. When velocities  $u(x, y, z)$  and  $v(x, y, z)$  are calculated in the time step  $n$ , the corresponding vertical velocity  $w(x, y, z)$  is computed by

$$w(x, y, z) = - \int_{l_k} u(x, y, z) dz - \int_{l_k} v(x, y, z) dz \quad (13)$$

The surface elevation  $\zeta$  is calculated by

$$\frac{\zeta^{n+1/2} - \zeta^{n-1/2}}{\Delta t} = - \frac{\partial(HU)^n}{\partial x} - \frac{\partial(HV)^n}{\partial y} \quad (14)$$

In the above-mentioned computation processes, the kinematic eddy viscosity  $\nu_t$  in the time-space domain has to be specified. Three types of turbulence models are incorporated into the numerical model for Q3-D storm surge prediction:

(1) For the zero-equation turbulence model,  $\nu_t$  is assumed as:

$$\nu_t = \text{constant} \quad \text{or} \quad \nu_t = l^2 \left| \frac{\partial u}{\partial z} \right| \quad (15)$$

(2) For the one-equation turbulence model,  $\nu_t$  is calculated as:

$$\nu_t = \sqrt{k} l \quad (16)$$

where  $l$  is the eddy length scale and  $k$  is calculated by the  $k$ -equation.

(3) For the two-equation turbulence model,  $\nu_t$  is calculated as:

$$\nu_t = C_D \frac{k^2}{\varepsilon} \tag{17}$$

where  $k$  and  $\varepsilon$  are obtained by the  $k$ - $\varepsilon$  model. Details of the  $k$ - $\varepsilon$  model are shown below.

The  $k$  equation is discretized by the Crank-Nicholson scheme as:

$$\begin{aligned} & \frac{k^{n+1}}{\Delta t} + \frac{1}{2} \left( w^n \frac{\partial k^{n+1}}{\partial z} \right) - \frac{1}{2} \left( \frac{\partial}{\partial z} \left( \frac{\nu_T}{\sigma_k} \frac{\partial k^{n+1}}{\partial z} \right) \right) \\ &= \frac{k^n}{\Delta t} - \frac{1}{2} \left( w^n \frac{\partial k^n}{\partial z} \right) + \frac{1}{2} \left( \frac{\partial}{\partial z} \left( \frac{\nu_T}{\sigma_k} \frac{\partial k^n}{\partial z} \right) \right) + P^n - \varepsilon^n \end{aligned} \tag{18}$$

The finite element formulation is made by multiplying the weighting function,  $\tilde{k}$ , to this equation and integrating it over the depth as:

$$\begin{aligned} & \int \tilde{k} \frac{k^{n+1}}{\Delta t} dz + \int \tilde{k} \left\{ \frac{1}{2} w^n \frac{\partial k^{n+1}}{\partial z} \right\} dz - \int \tilde{k} \left\{ \frac{1}{2} \frac{\partial}{\partial z} \left( \frac{\nu_T}{\sigma_k} \frac{\partial k^{n+1}}{\partial z} \right) \right\} dz = \int \tilde{k} \frac{k^n}{\Delta t} dz \\ & - \int \tilde{k} \left\{ \frac{1}{2} w^n \frac{\partial k^n}{\partial z} \right\} dz + \int \tilde{k} \left\{ \frac{1}{2} \frac{\partial}{\partial z} \left( \frac{\nu_T}{\sigma_k} \frac{\partial k^n}{\partial z} \right) \right\} dz + \int \tilde{k} P^n dz - \int \tilde{k} \varepsilon^n dz \end{aligned} \tag{19}$$

The linear shape function, Eq. (20), is assumed in the finite element formulation.

$$N_k = \frac{1}{l_k}(z_{k+1} - z), \quad N_{k+1} = \frac{1}{l_k}(z - z_k) \tag{20}$$

where  $k$  is the nodal number,  $l_k$  the element length, and  $z_k$  the position of  $k$  in the  $z$  axis.

The point of  $z$  is interpolated by,

$$z = N_k z_k + N_{k+1} z_{k+1} \tag{21}$$

Applying the Galerkin method, the integrations of each term in the equation are shown respectively as:

Equations for  $\varepsilon$  are derived in the same manner, and are solved numerically together with the  $k$  equations by the Gaussian elimination method.

Fundamental Tests of Q3-D Model

Model parameters in the  $k$ - $\varepsilon$  equations will now be discussed along with several fundamental tests in the rectangular flume (i.e. swing and wind-induced current tests).

**Boundary conditions at the bottom and surface:** For time-averaging turbulence models, such as the  $k$ - $\varepsilon$  and one equation models, the boundary conditions at the bottom and surface have to be carefully discussed because of its strong

shear flow characteristics. Usual modeling method in this area apply the knowledge called the universal law of the wall, which depicts the velocity distribution of shear flow by a logarithmic law given by

$$\frac{u}{u_\tau} = \frac{1}{\kappa} \ln \frac{E u_\tau y}{\nu} \quad (22)$$

where  $u_\tau$  is the friction velocity,  $\kappa$  the Kármán constant,  $E$  the roughness parameter,  $y$  the distance from the wall, and  $\nu$  the kinematic viscosity of the fluid. When we assume a hydraulically smooth wall, the roughness parameter may be evaluated by  $E = 9$  in the range of  $30 < u_\tau y / \nu < 100$ . This concept is useful in the modeling of mean flow field in the boundary layer. Equation (22) is used to develop a quasi-three dimensional model for simulation of storm surges.

On the other hand, the boundary condition of the turbulence model is posed by the assumption of balancing production and dissipation, which results in the following relation

$$\frac{k}{u_\tau^2} = \frac{1}{\sqrt{c_\mu}}, \quad \varepsilon = \frac{u_\tau^3}{\kappa y} \quad (23)$$

for the  $k$ - $\varepsilon$  model.

To compute the mean flow in the interior region, we have to specify the velocity at the interface between the interior region and boundary layer with the relation of shear stresses and eddy viscosity given respectively by

$$\left( \nu_t \frac{\partial u}{\partial z} \right)_{z=\zeta} = \tau_s \quad \text{at the surface} \quad (24)$$

$$\left( \nu_t \frac{\partial u}{\partial z} \right)_{z=-h} = \tau_b \quad \text{at the bottom} \quad (25)$$

where  $\tau_s$  and  $\tau_b$  are the shear stresses at the surface and bottom of the sea respectively.

When we specify the shear stresses ( $\tau_s$  and  $\tau_b$ ), and turbulence properties ( $k$  and  $\varepsilon$ ), it is possible to get the boundary condition for mean flow field by velocity gradient. The following relation is used to evaluate the eddy viscosity,  $\nu_t$ .

$$\nu_t = c_\mu \frac{k^2}{\varepsilon} \quad (26)$$

Dirichlet's problem for the discrete system brings a difficulty in determining the velocity gradient without dependence on grid size. Fine mesh makes the model extremely expensive in the three-dimensional case. To overcome these problems the point where the boundary condition is posed is fixed in this investigation. At the surface layer the point of  $\Delta z_s = 1.35\text{m}$  and  $\Delta z_b = 0.1\text{m}$  at the bottom are set. This means that the distance from the bottom or surface,  $y$ , is fixed by  $\Delta z_s$  or  $\Delta z_b$  in the wall law relation of Eq.(22) or Eq.(23). In the case of the zero-equation turbulence model we do not have any information about turbulence near the boundary, therefore we need some assumptions in evaluating the eddy viscosity  $\nu_t$  or shear stresses  $\tau_b$  and/or  $\tau_s$ . If the two-equation turbulence model is used, we do not need any assumption. We do need much CPU time and information of turbulence at the open boundary. This is usually difficult to get.

For zero-equation modeling, the following text elaborates on the way to determine the bottom shear stresses from the numerical results of swing and wind-induced current tests. For this purpose, both the quasi-three dimensional simulation of  $k-\epsilon$  model version and the horizontally two-dimensional simulation are also conducted under the same computational condition. These results are used as indexes to determine the bottom shear stresses at the fixed point  $\Delta z_b$  by comparison of surface elevations. Moreover, a simulation of flow combined tides and wind-induced currents is performed by the model of zero-equation turbulent version.

**Swing test** Free oscillation of water in the closed flume may be simulated fairly well by the so-called single level model (horizontally two-dimensional model). By comparing the water surface oscillations computed by the single level model and those by the Q3-D model, the bottom shear stress of Q3-D model can be evaluated. As previously stated, this is one of the parameters which has to be determined in the Q3-D model. A closed flume which is used for the swing test has a dimensions of uniform water depth of 20 m deep,  $L=10,000$  m in length and  $B=3,000$  m in width. The horizontal spacing of the grid system is  $\Delta x=1000$  m and the number of the vertical nodes is 35. Time increment is fixed by  $\Delta t=10$  sec. The initial surface profile is given by  $\zeta(x) = 0.0001x - 0.5$ . For the zero-equation version of Q3-D model, the vertical distribution of eddy viscosity is assumed by the following equation which is obtained by fitting the mean velocity distribution with Baines and Knapp's experiment.

$$\nu_t = 0.01 + \kappa C_\mu \left(1 - 3.6 \frac{z}{h}\right) \frac{z}{h} \quad (27)$$

This assumption of eddy viscosity distribution will be further discussed later by comparing zero and two equation models in  $\nu_t(z)$ .

Surface elevation at the right end is shown in Figure 2 together with the results computed by the leap-frog scheme(dotted line). Bottom friction is neglected in the computation by leap-frog scheme. The computed propagation speed of the disturbance on the uniform depth of 20 m is 1428 sec, which is equivalent to the long wave celerity. It can be recognized that almost uniform velocity distribution of the mean current is computed in the case of swing test with no bottom friction.

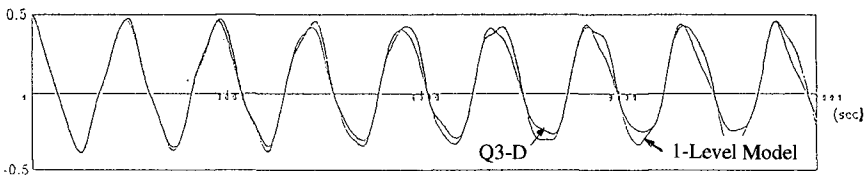


Figure 2 Comparison of water surface oscillation at the flume computed by Q3-D model (solid line) and 1-Level Model (dotted line).

**Wind-induced current test** The three-dimensional model is of course more effective than the horizontally two-dimensional in the computation of wind induced current which is characterized by the strong shear near the surface. In the case of a closed basin, a return flow is observed near the bottom.

A wind-induced flow test in the closed flume is conducted and the vertical distribution of eddy viscosity as well as mean flow is discussed together with surface elevation property. This is calibrated by a comparison with theoretical formulation of wind set-up using Eq. (28).

$$\zeta_{\max} = \frac{3\rho_a C_D L W^2}{4g D \rho_w} \tag{28}$$

where  $\zeta_{\max}$  is the maximum water surface elevation,  $C_D$  the drag coefficient at the surface,  $L$  length of the flume,  $W$  the wind velocity,  $D$  the total depth,  $\rho_a$  the density of air, and  $\rho_w$  the density of sea water.

As mentioned before, shearing stresses both at the surface and bottom are not uniquely determined in the Q3-D model of the zero-equation version of turbulence. They depend on the spacing of nodes just inside the interface because an approximation accuracy of the mean flow gradient depends on node spacing. When the number of vertical node points is fixed, shearing stresses are dependent upon the total depth. Figure 3 depicts this effect, in which four different results in the maximum surface elevation under the same condition are compared. Changing the still water depth in the range of 5 to 40 m, the maximum wind set-up is computed under the condition of uniform wind speed of 20 m/sec in the same flume as swing test. Gradually increasing wind speed from 0 to 20 m/sec for 3000 sec is assumed in the test to reduce time to be steady state which means small tank oscillation is expected. In the figure, Q3-D CONST indicates the results computed by using the uniform distribution of eddy viscosity in the Q3-D model of zero-equation turbulence version, Q3-D QUARD indicates those expressed by the distribution resulting from Eq. (27), 1LEVEL MODEL indicates those developed by the horizontally two dimensional model.

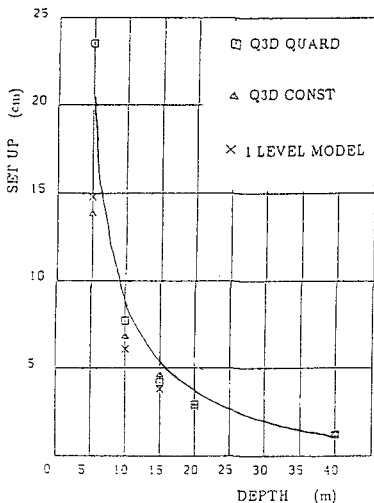


Figure 3 Relation between the water depth and the computed set-up.

It can be recognized that the wind set-up computed by Q3-D QUARD is larger than that computed by other models in the region shallower than 10 to 5 m. This means that it may result in over-estimate of the shearing stress at the surface, and

a lower-estimate at the bottom in the very shallow region, because the their real distribution may become uniform as the depth becomes shallower. The difference between 1LEVEL MODEL and the solid line comes from the difference of out-put points. The out-put point of numerical computation is just inside of the end-wall.

Vertical distributions of the mean flow and eddy viscosity at the center of the flume in steady state is shown in Figure 4 where the column is the depth nondimensionarized by the still water depth, while the abscissas indicates the horizontal velocity normalized by friction velocity. White circles in the figure indicate the experimental values of Baines-Knapp showing the null-velocity point at 0.7 in nondimensional depth.

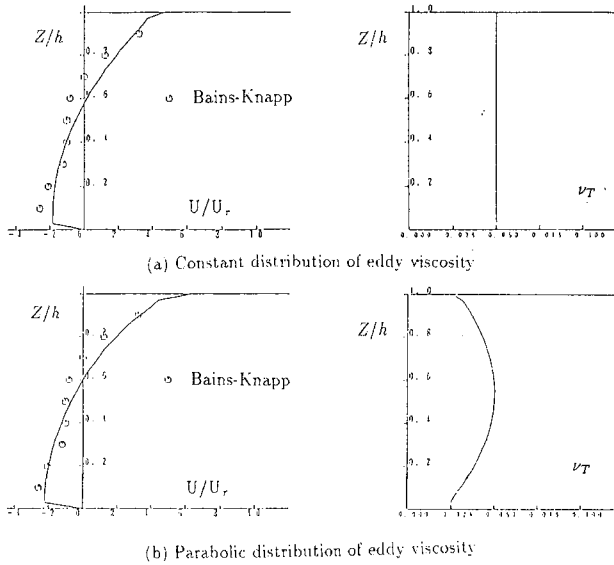


Figure 4 Vertical distribution of the mean flow and eddy viscosity at the center of the flume in steady state by Q3-D model of zero-equation turbulence version.

On the other hand, Figure 5 also shows the vertical distribution of both mean flow velocity and eddy viscosity which were computed in terms of the Q3-D model of  $k-\epsilon$  version whose boundary conditions are given by Eq. (23) for  $k$  and Eq. (29) for  $\epsilon$ .

$$\epsilon_s = \frac{k_s^{\frac{3}{2}}}{\kappa L_s}, \quad \epsilon_b = \frac{k_b^{\frac{3}{2}}}{\kappa L_b} \tag{29}$$

where the length scale parameters are assumed as  $L_s = 100\Delta z_s$  and  $L_b = \Delta z_b$  by comparison of mean flow velocity distribution with Baines and Knapp's experiments.

From these figures it is found that the null-velocity point of the vertical distribution of mean flow is located around the nondimensional depth of 0.6 which is slightly lower than that by experiment. Moreover the vertical distribution of computed eddy viscosity by the  $k-\epsilon$  model is similar to that of a parabola,

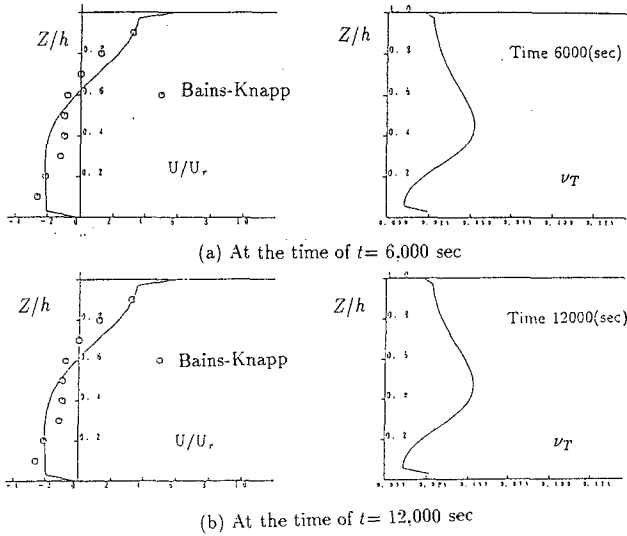


Figure 5 Vertical distributions of the mean flow and eddy viscosity at the center of the flume in steady state by Q3-D model of  $k-\epsilon$  version.

Eq. (27), which is assumed for the model of zero-equation version. The computed eddy viscosity, however, skews downward with its maximum at 0.4 in the nondimensional depth.

Application to wind-induced currents in Tanabe Bay

Observations of vertical velocity distribution in terms of an acoustic Doppler current profiler (ADCP) have been conducted since 1989 in Tanabe Bay by the Shirahama Oceanographic Observatory, Disaster Prevention Research Institute, Kyoto University. Tide and wind vector on the sea surface are also observed at the Oceanographical observation tower whose location is indicated in the map of Tanabe Bay (Figure 6) together with ADCP's location and depth contours.

As this data is very useful for calibration of three-dimensional numerical model, simulation tests of mean flow in Tanabe Bay are carried out to compare with observation in the current profile. Because the model assumes a well-mixed situation in the sea, the observed profile of mean current of horizontal component in winter season is selected for comparison. Figure 7 shows the time changes in wind vector(upper), tide(middle) and current profile(bottom) which are used for model calibration here. Current vector in this figure is defined by NS-WE system in which the northward component is plotted upward and the westward current is leftward. A typical feature of this data is the strong wind-induced currents whose direction is ESE and the return flow to the direction of W.

The sea bottom topography is reproduced from the chart (No. 74) with the grid system of  $\Delta x = 100$  m. Total point number is  $89 \times 110$  and the origin is  $33^\circ 44' 40''$  north latitude and  $135^\circ 17' 00''$  east longitude. For actual computation, 200m horizontal grid size, 19-point vertical nodal points, and 5sec time increment

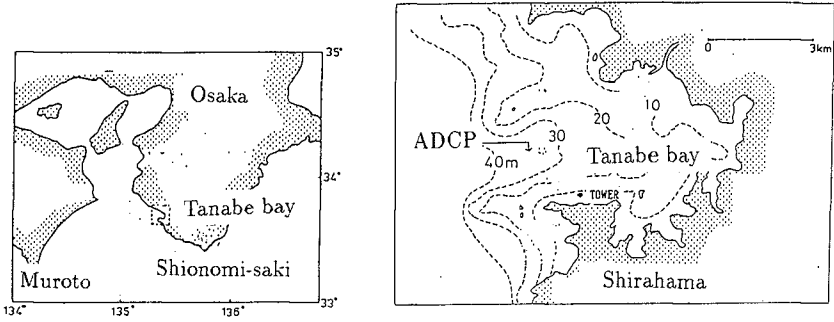


Figure 6 Location of the Tanabe Bay and the oceanographical observation tower together with ADCP's observation point.

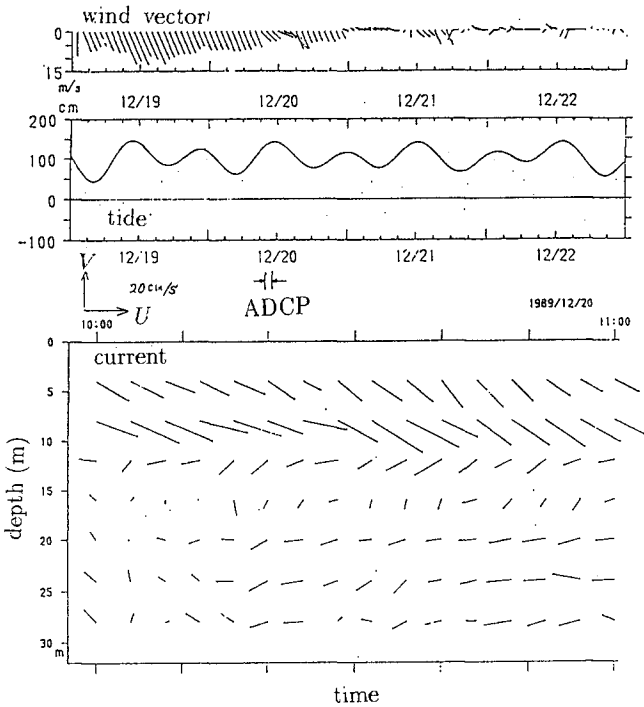


Figure 7 The data of wind vector(upper), tide(middle) and current profile(bottom), observed on December 12, 1989.



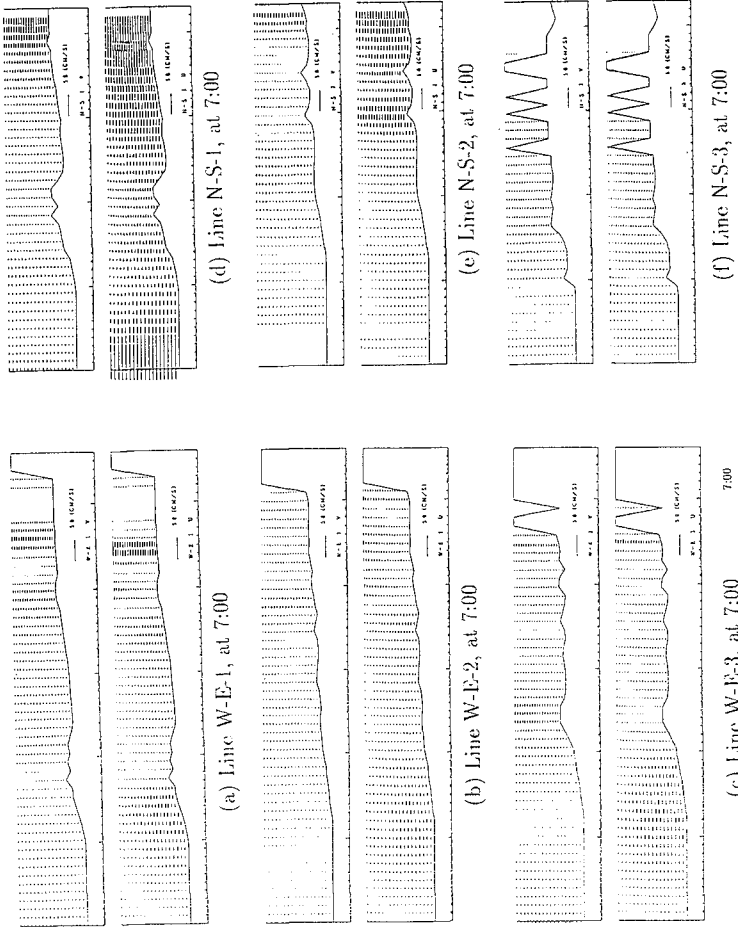
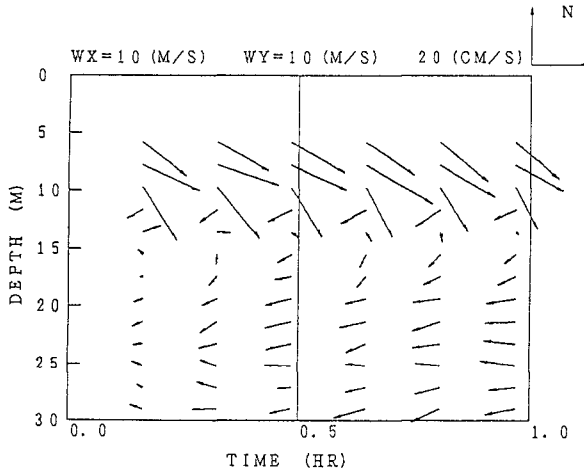
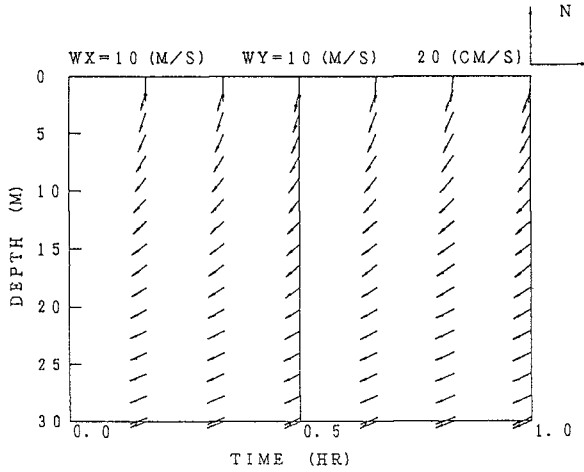


Figure 9 Current profile distribution on the observation lines of N-S-1, N-S-2, N-S-3, W-E-1, W-E-2 and W-E-3.



(a) Observed velocity profile by ADCP



(b) Computed velocity profile by Q-3D model

Figure 10 Comparison between observation and simulation of current profile. Observation of 2 min and 10 min averaging and computation output of 10 min interval.

are employed. Simulation period is 5:00-11:00, 20 December, 1989 which covers ADCP observation, 10:00-11:00. Wind condition is assumed to be constant NW wind whose velocity is 10 m/sec.

A sample of the computed mean flow vectors at the surface level, 5m level, 10m level and 30m level are shown in Figure 8. The vertical velocity distribution on six lines of N-S-1, N-S-2, N-S-3, W-E-1, W-E-2 and W-E-3 are shown in Figure 9. Figure 10 is the comparison between observation and simulation, in which observation of 2 min and 10 min averaging and computation output of 10 min interval are shown. The strong wind-induced flow is not simulated in the numerical model, however, the return flow (probably the tidal current) is well simulated both in its magnitude and direction. One possibility which may cause this discrepancy may be the open boundary condition. The other may be some trouble in the ADCP observation. Further discussion about this will be needed in terms of continuous efforts in executing simulations and ADCP observations.

### Conclusions

A three-dimensional model for storm surges was developed and its fundamental tests were carried out. The obtained main results in this paper are shown below.

(1) From the swing test, propagation speed of the initial disturbance was confirmed to be in good agreement with that of free long waves.

(2) From the wind-induced current test in the two-dimensional flume, it was found by fitting the mean velocity profile with the Baines and Knapp's experiment that the eddy viscosity  $\nu_t$  was around 0.01-0.02 m<sup>2</sup>/s for Q3-D model of zero-equation version. Moreover the profile of eddy viscosity computed by the  $k$ - $\epsilon$  model was similar to that assumed the parabolic profile in the zero-equation version.

(3) The simulation of the flow fields in the Tanabe Bay was performed, in which both tides and wind-induced currents were taken into consideration. The velocity profile observation with ADCP also was conducted in the bay. From the comparison of velocity profile between observations and computations, it was found that the strong surface wind-induced flow was not simulated, however the return flow was well simulated both in its magnitude and direction.

### References

- Hansen, W.(1962), Hydrodynamical methods applied to oceanographic problems, Mitt. Inst. Meereskd., University of Hamburg, Hamburg.
- Heaps, N.S.(1973), Three-dimensional model of the Irish Sea, Geophys. J. R. Astron. Soc., Vol.35, pp.99-120.
- Koutitas, C. and B.A. O'Connor(1980), Modeling three-dimensional wind-induced flow, Proc. ASCE, Jour. Hydraulics Div., Vol.106, HY11, pp.1843-1865.
- Laevastu, T.(1975), Multilayer hydrodynamical-numerical models, Proc. Symp. Modelling Tech., ASCE, p.1010.
- Simons, T.J.(1974), Verification of numerical models of Lake Ontario: Part I. Circulation in spring and early summer, Jour. Phys. Oceanogr., Vol.4, p.507.
- Simons, T.J.(1975), Verification of numerical models of Lake Ontario: Part II. Stratified circulation and temperature changes, Jour. Phys. Oceanogr., Vol.5, pp.98-110.
- Sundermann, J.(1974), A three-dimensional model of a homogeneous estuary, Proc. 14th ICCE, ACSE, pp.2337-2390.

